DET1-mediated degradation of a SAGA-like deubiquitination module controls H2Bub homeostasis

Amr Nassrallah[a,§,#], Martin Rougée[b,c,#], Clara Bourbousse[b,c], Stéphanie Drevensek[b,‡], Sandra Fonseca[a], Elisa Iniesto[a,¶], Ouardia Ait-Mohamed[b], Anne-Flore Deton-Cabanillas[b], Gerald Zabulon[b], Ikhlak Ahmed[b,†], David Stroebel[b], Vanessa Masson[d], Bérangère Lombard[d], Dominique Eeckhout[e,f], Kris Gevaert[g,h], Damarys Loew[d], Auguste Genovesio[b], Cécile Breyton[i], Geert de Jaeger[e,f], Chris Bowler[b]*, Vicente Rubio[a]* and Fredy Barneche[b]*

[a]Centro Nacional de Biotecnología (CNB-CSIC) Darwin 3, 28049 Madrid, Spain
[b]Institut de biologie de l'Ecole normale supérieure (IBENS), Ecole normale supérieure, CNRS, INSERM, PSL Université Paris 75005 Paris, France.
[c]Université Paris-Sud, 91405 Orsay, France
[d]Institut Curie, PSL Research University, Centre de Recherche, Laboratoire de Spectrométrie de Masse Protéomique, 26 rue d'Ulm, 75005 Paris, France
[e]Department of Plant Systems Biology. VIB-Ghent University. Technologiepark 927, B-9052 Ghent, Belgium
[f]VIB Center for Plant Systems Biology, 9052 Ghent, Belgium
[g]Department of Biochemistry, Ghent University, 9000 Ghent, Belgium
[h]VIB Center for Medical Biotechnology, 9000 Ghent, Belgium
[i]Université Grenoble Alpes, CNRS, CEA, Institut de Biologie Structurale (IBS), F-3800, Grenoble, France
[§]Present address: Biochemistry Department, Faculty of Agriculture, Cairo University, Giza 12613, Egypt
[¶]Present address: Salk Institute for Biological Studies, 10010 N Torrey Pines Rd, La Jolla, CA 92037 USA
[†]Present address: Weill Cornell Medicine - Qatar (WCM-Q) Education City, P.O. Box 24144, Doha, Qatar
[‡]Present address: Institut of Plant Sciences Paris-Saclay (IPS2), UMR 9213/UMR1403, CNRS, INRA, Université Paris-Sud, Université d'Evry, Université Paris-Diderot, Sorbonne Paris-Cité, Orsay, France
[#]Equal contribution
*Correspondence: barneche@biologie.ens.fr, vrubio@cnb.csic.es or cbowler@biologie.ens.fr

Keywords: Epigenome, Histone H2B deubiquitination; Light signaling; DET1; SAGA complex; Arabidopsis

Summary

DE-ETIOLATED 1 (DET1) is an evolutionarily conserved component of the ubiquitination machinery that mediates the destabilization of key regulators of cell differentiation and proliferation in multicellular organisms. In this study, we provide evidence from Arabidopsis that DET1 is essential for the regulation of histone H2B monoubiquitination (H2Bub) over most genes by controlling the stability of a plant deubiquitination module (DUBm). In contrast with yeast and metazoan DUB modules that are associated with the large SAGA complex, the Arabidopsis DUBm only comprises three proteins (hereafter named SGF11, ENY2 and UBP22) and appears to act independently as a major H2Bub deubiquitinase activity. Our study further unveils that DET1-DDB1-Associated-1 (DDA1) protein interacts with SGF11 *in vivo*, linking the DET1 complex to light-dependent ubiquitin-mediated proteolytic degradation of the DUBm. Collectively, these findings uncover a signaling path controlling DUBm availability, potentially adjusting H2Bub turnover capacity to the cell transcriptional status.

Introduction

DE-ETIOLATED 1 (DET1) is an evolutionarily conserved factor in multicellular organisms, acting in most instances to regulate gene expression through ubiquitin-mediated protein degradation. *DET1* null mutations are lethal in plants (Misera et al., 1994; Pepper et al., 1994), Drosophila (Berloco et al., 2001) and Human (Wertz et al., 2004). However, viable Arabidopsis knockdown alleles identified in genetic screens for mutant plants displaying a constitutive photomorphogenic phenotype (i.e. de-etiolated) have unveiled that DET1 is a central integrator of light signaling in plants (Chory et al., 1989; Pepper et al., 1994). The Arabidopsis *det1-1* mutation affects the

expression of thousands of nuclear genes (Ma et al., 2003; Schroeder et al., 2002), partly because proteolytic degradation of the proto-photomorphogenic transcription factor HY5 is abolished in this background, thereby mimicking the presence of light on the transcriptional program (Osterlund et al., 2000). In humans, DET1 also controls the stability of cell proliferation factors such as the Cdt1 DNA replication-licensing factor (Pick et al., 2007) and the proto-oncogenic transcription factor c-Jun (Wertz et al., 2004). Accordingly, a currently accepted model in both plants and animals is that DET1 is an atypical DDB1-CULLIN4 Associated Factor (DCAF) acting with the small DDA1 (DET1-DDBA1-Associated 1) protein to provide specificity to one or more E3 CULLIN4-RING ubiquitin ligases (CRL4) (Chory, 2010; Lau and Deng, 2012). For this activity, DET1 and DDA1, together with the DDB1 and COP10 proteins, constitute a substrate adaptor module (COP10-DET1-DDB1-DDA1; hereafter termed C3D) within CRL4 complexes (Irigoyen et al., 2014; Pick et al., 2007).

Photomorphogenesis is a developmental switch that initiates upon the first perception of light by young plants reaching the soil surface. This transition triggers the launching of organ growth and the establishment of photosynthesis, most notably through the differentiation of primary leaf (cotyledon) cells (reviewed in (Casal, 2013; Seluzicki et al., 2017; Wu, 2014). The process involves changes at transcriptomic, epigenomic and nuclear architecture levels (Bourbousse et al., 2015; Charron et al., 2009; Sullivan et al., 2014). While several chromatin modifiers are known to influence light-responsive gene expression, the first direct link between light signaling and chromatin came from the discovery that DET1 has high affinity for nucleosomal histone H2B *in vitro* and *in vivo* (Benvenuto et al., 2002). By potentially being at the interface between light signaling and epigenome dynamics, a chromatin-level function of DET1 in photomorphogenesis has long been proposed (Chory, 2010; Lau and Deng, 2012), yet the chain of events leading from light sensing to epigenomic reprogramming is still largely ignored (reviewed in (Barneche et al., 2014; Perrella and Kaiserli, 2016)). Here, we unveil a direct link between DET1 and the histone H2B monoubiquitination pathway. This histone post-translational modification (PTM) acts cooperatively with RNA Polymerase II (RNA Pol II) and other PTMs of histones to promote gene expression and the regulation of cellular homeostasis in various organisms (Shema et al., 2008; Smith and Shilatifard, 2013; Weake and Workman, 2011).

Transcription-coupled chromatin remodeling and modification play a fundamental role in the fine-tuning of genome expression. In the sequence of events established in the yeast *Saccharomyces cerevisiae*, the Polymerase-associated factor 1 (PAF1) complex interacts with Ser-5 phosphorylated RNA Pol II and serves as a platform for H2B monoubiquitination by the Rad6 E2 ubiquitin conjugase and the Bre1 E3 ligase. In turn, recruitment of the SAGA (Spt-Ada-Gcn5-acetyltransferase) complex at the Pre-Initiation Complex (PIC) triggers H2Bub de-ubiquitination and phosphorylation of Pol II CTD on Ser-2, mediating the transition towards transcription elongation (Wyce et al., 2007). Sliding from the promoter, SAGA is thought to travel along the gene body with RNA Pol II to allow for repeated cycles of histone H2B ubiquitination/de-ubiquitination by opposing Bre1 activity (Henry et al., 2003). This is thought to facilitate the progression of RNA Pol II through nucleosomal barriers by influencing DNA accessibility, recruitment of the histone chaperone FACT (FAcilitates Chromatin Transcription) and promoting nucleosome reassembly (Belotserkovskaya et al., 2003; Fierz et al., 2011; Fleming et al., 2008; Pavri et al., 2006; Xin et al., 2009). Accordingly, SAGA displays a general co-activator activity that promotes transcription at a post-initiation step on most expressed genes in budding yeast (Baptista et al., 2017; Bonnet et al., 2014), with a pronounced effect on so-called SAGA-bound "regulatable" genes (de Jonge et al., 2017).

In budding yeast and metazoans, SAGA is a ~1.8 megaDa gigantic complex made of functionally distinct components comprising a TBP-associated factor (TAF) architectural core module, a TATA-Binding Protein (TBP) module, a histone acetyltransferase (HAT) module, and a H2Bub deubiquitination module (DUBm) (Grant et al., 1997). DUBm is an independent structure that functionally requires the Ubiquitin protease 8 (Ubp8) catalytic subunit, the Sgf11 (SAGA-associated factor 11) nucleosome-binding subunit and the small protein Sus1 (Sl gene upstream of ySa1), which binds ubiquitin (Rodriguez-Navarro, 2009), while the fourth subunit Sgf73 makes the bridge with core SAGA modules (Kohler et al., 2008; Lee et al., 2009).

Despite the functional conservation of the SAGA central core subunit ADA2b and the GCN5 histone acetyltransferase (Benhamed et al., 2006; Vlachonasios et al., 2003), a structural and functional

characterization of plant SAGA complexes is still missing. Orthologous proteins of Ubp8, Sgf11 and Sus1 or their human counterparts USP22, ATXN7L3 and ENY2 have been identified from the genome sequence of *Arabidopsis thaliana* model species but Sgf73 appears to be absent (Moraga and Aquea, 2015; Srivastava et al., 2015). Arabidopsis UBIQUITIN PROTEASE 26 (UBP26) deubiquitinates H2Bub *in vivo*, impacting expression of the *FLC* developmental regulator (Schmitz et al., 2009), but it appears to act independently from SAGA and rather displays a repressive activity on transposable elements (Sridhar et al., 2007) and imprinted genes (Luo et al., 2008). More generally, homolog proteins of SAGA, Bre1, PAF1c and COMPASS subunits are known to influence plant development and responses to biotic and abiotic stress, (Grasser and Grasser, 2017; Moraga and Aquea, 2015; Van Lijsebettens and Grasser, 2014), but the structure and function of transcription co-activators, their influence on gene activity and on how they are themselves regulated during cell specialization and adaptation largely remain to be characterized in plant systems. Recent purification of elongating RNA Pol II has indeed shown its tight association with chromatin machineries such as PAF1, FACT and HUB complex subunits in Arabidopsis (Antosz et al., 2017). HUB is the only known histone H2B E3 ubiquitin ligase in Arabidopsis, acting as a heterotetramer of the HISTONE UBIQUITINATION 1 (HUB1) and HUB2 proteins (reviewed in (Feng and Shen, 2014)). Although null mutations in *HUB1* or *HUB2* genes abolish H2Bub deposition, knockout plants are viable with only mild phenotypic defects in seed dormancy, cell cycle progression, circadian clock and flowering time control (Cao et al., 2008; Fleury et al., 2007; Liu et al., 2007). Still, abrogating *HUB1* function impairs rapid modulation of RNA levels of light-regulated genes during seedling photomorphogenesis, suggesting that monoubiquitinated H2B is required to attain high expression levels during Arabidopsis photomorphogenesis (Bourbousse et al., 2012).

In this study, we first provide evidence that DET1 is essential for the regulation of H2Bub levels over most genes by controlling the light-dependent degradation of a plant H2Bub deubiquitination module (DUBm). This DUBm comprises SGF11, UBP22 and ENY2, the Arabidopsis orthologous proteins of yeast Sgf11, Ubp8 and Sus1, respectively, which, in the absence of a predictable plant Sgf73-like subunit, appears to act independently from SAGA. Although the Arabidopsis genome encodes 14 families of ubiquitin-proteases, altogether representing 27 members (March and Farrona, 2017), *UBP22* loss-of-function drastically impairs H2Bub removal, indicating its major H2Bub deubiquitinase activity in Arabidopsis. Our study further reveals that Arabidopsis SGF11 physically links DUBm to the DDA1 C3D subunit *in vivo* and is subject to DET1-dependent ubiquitin-mediated degradation. Collectively, this study uncovers a signaling path controlling global H2Bub levels, potentially fine-tuning gene transcriptional capacity or "regulatability" during developmental responses to external cues.

Results

DET1 is required for H2Bub enrichment over most genes

To investigate how DET1 impacts on chromatin status, we tested whether histone post-translational modifications (PTMs) were affected in *det1-1* mutant plants by conducting label-free quantitative mass spectrometry analysis of purified histones (Figure S1). We identified 15 different peptide sequences bearing one or more differentially modified residues in *det1-1* seedlings, half of them matching histone H2B (Table S1). Histone H2B was found to be more frequently acetylated and twice less monoubiquitinated at a conserved lysine residue in the carboxy-terminal tail of 9 different H2B isoforms (Figures 1A-B and S1B). Low H2Bub levels in these mutant plants were reproducibly visualized by immunoblot detection using an antibody that recognizes H2B histone isoforms and their slower migrating monoubiquitinated forms in chromatin-enriched samples (Figure 1C and 1D). This defect was also confirmed by immunoprecipitation of MYC-tagged ubiquitin proteins from wild-type and *det1-1* plants followed by detection of histone H2B proteins (Figure S1C). Finally, introgression of the *hub1-3* mutation in the *det1-1* genetic background indicated that remaining H2Bub marks in *det1-1* plants are deposited via the HUB pathway (Figure 1D). The mass spectrometry analysis also indicated an increase of histone H3 methylation on Lys-27 or Lys-36, but no robust differences in H3K36me3 or H3K27me3 could be detected by immunoblot analysis (Figure 1C). Instead, complementary immunoblot analyses of euchromatic histone marks detected increased H3K9ac levels and reduction of H3K27ac levels in *det1-1* (Figure 1C), which had not been found by mass spectrometry.

A

Histone type	Peptide sequence	Histone PTM position(s)	*det1-1* / WT
H2A.Z	GA**K**GLIMGKPSGSDKDKDK	Ac (K6)	4.44
H2A.Z	BG**K**GG**K**GLVAAK	Ac (Nter or K3 K6)	2.27
H2B	AVT**K**FTSS	Ub (K122 to 145)	0.47
H2B	AG**K**KPAE**K**KPAE**K**APAEEEK	Ac (K6 K11 K16)	11.92
H2B	KPAE**K**KPAE**K**APAEEEK	Ac (K11 K16)	6.46
H2B	VAE**K**APAE**KK**PK	Ac (K27 K32 or 33)-1	4.05
H2A	G**K**TLGSGVAK	Ac (K5)	3.43
H2B	AAE**K**APAE**K**KPK	Ac (K27 K32)	2.44
H2A	G**K**QLGSGAAK	Ac (K5)	2.38
H2B	APAEEEKVAE**K**APAE**KK**PK	Ac (K27 K32 or 33)-2	2.31
H2B	AE**K**APAE**K**KPK	Ac (K27 K32)-1	2.12
H3.3	**K**SAPTTGGV**KK**PHR	4Me (K27 or 36 or 37)	2.19
H3.3	SAPTTGGV**K**KPHR	me2 (K36)	2.07
H3.3	**K**SAPTTGGV**K**KPHR	3Me (K27 or 36)	2.01
H3.3	**K**SAPTTGGV**KK**PHR	Me (K27) + Ac (K36 or	2.01
H3.1	SAPATGGV**K**KPHR	me2 (K36)	2.03

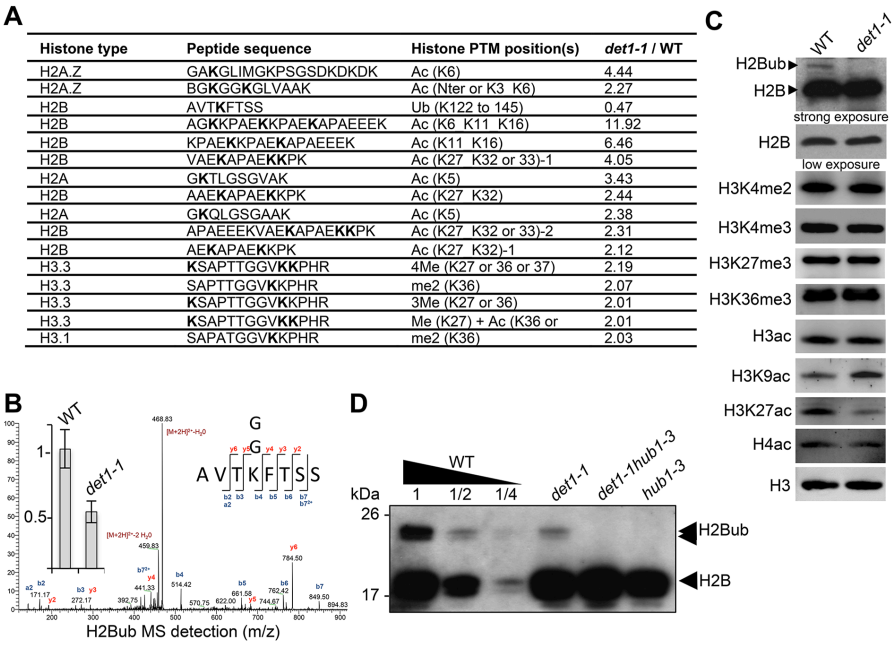

Figure 1. *DET1* loss-of-function triggers a massive reduction of H2Bub.
(A) Mass spectrometry detection of differentially modified histones using non-modified histone peptides as internal references. Differentially modified residues are shown in bold. Several candidate residues are bolded when the precise position of the differentially modified residue could not be determined. Only significantly modified peptides from 3 biological replicates are shown (p-Val<0.001; >2-fold change). Histone isoforms were annotated according to Talbert et al. (2012). Ac, acetylation; Ub, ubiquitination; Me, methylation; xMe: x methylations on a unique or distinct residues; me1, monomethylation; me2, dimethylation; me3, trimethylation. **(B)** Representative MS/MS spectra of histone H2B monoubiquitination at a the conserved lysine residue in the AVTKubFTSS peptide known to be monoubiquitinated in plants (Bergmuller et al., 2007; Sridhar et al., 2007). The fragmentation spectrum is derived from a trypsin-digested position matching the HTB1/2/3/4/6/7/9/10/11 isoforms. The ubiquitinated peptide sequence and observed ions are indicated on top of spectra. Singly and doubly charged a, b and y ions, as well as ions corresponding to neutral losses of water and NH3 groups; M, parent ion mass are shown. The inset shows the relative abundance of the monoubiquitinated AVTKFTSS peptide in wild-type (arbitrarily set to 1) and *det1-1* mutant plants. Intensity is calculated as the normalized average integrated MS peak area of the modified peptide from three independent biological replicates for each plant line. Data are represented as mean with 5% confidence interval. More details are given in the Experimental Procedures. **(C)** Immunoblot analysis of chromatin extracts from wild-type and *det1-1* seedlings performed with the indicated antibodies. **(D)** Immunoblot analysis of H2Bub in *det1-1* mutant seedlings, performed as in (C). Identity of the H2Bub band is confirmed by co-migration of *hub1-3* mutant chromatin extracts. In (C-D), the anti-H2B antibody allows detecting simultaneously core histone H2B (18kDa) and monoubiquitinated (~24 kDa) H2B forms.

Given the affinity of DET1 for histone H2B (Benvenuto et al., 2002) and its implication in the ubiquitination pathway (Osterlund et al., 2000; Yanagawa et al., 2004), we focused on the reduction of H2Bub levels in *det1-1* seedlings. We first assessed on which loci DET1 impacted the genomic landscape of this chromatin mark by conducting a H2Bub ChIP-seq analysis of wild-type and *det1-1* mutant seedlings grown under dark or light conditions. To allow for quantitative comparisons of differential enrichments in samples displaying drastic differences in H2Bub abundance, 3% Drosophila chromatin was spiked in each input, and *ad hoc* normalization of the Input/IP signals was performed for each sample individually (modified from the original ChIP with reference exogenous genome ChIP-Rx protocol from (Orlando et al., 2014); see Experimental Procedures). Consistent with our previous findings obtained by ChIP-chip (Bourbousse et al., 2012; Roudier et al., 2011), H2Bub domains were largely restricted to the transcribed regions. While a set of ~6,900 genes consistently bear a H2Bub peak in all four samples, the number of marked genes in *det1-1* compared to WT plants was 19% lower in the light (2,134 fewer genes) and 26% lower in the dark (2,577 fewer genes) (Figure 2A). Quantification using Rx scaling factors unveiled a severe decrease of H2Bub average level over the set of marked genes in *det1-1* seedlings, which was similarly observed in both light conditions (Figure 2B-C). Identification of the H2Bub-marked genes that are differentially ubiquitinated (DUGs) further showed that H2Bub is decreased over almost all genes in *det1-1* plants, regardless of the light condition (Figure 2D).

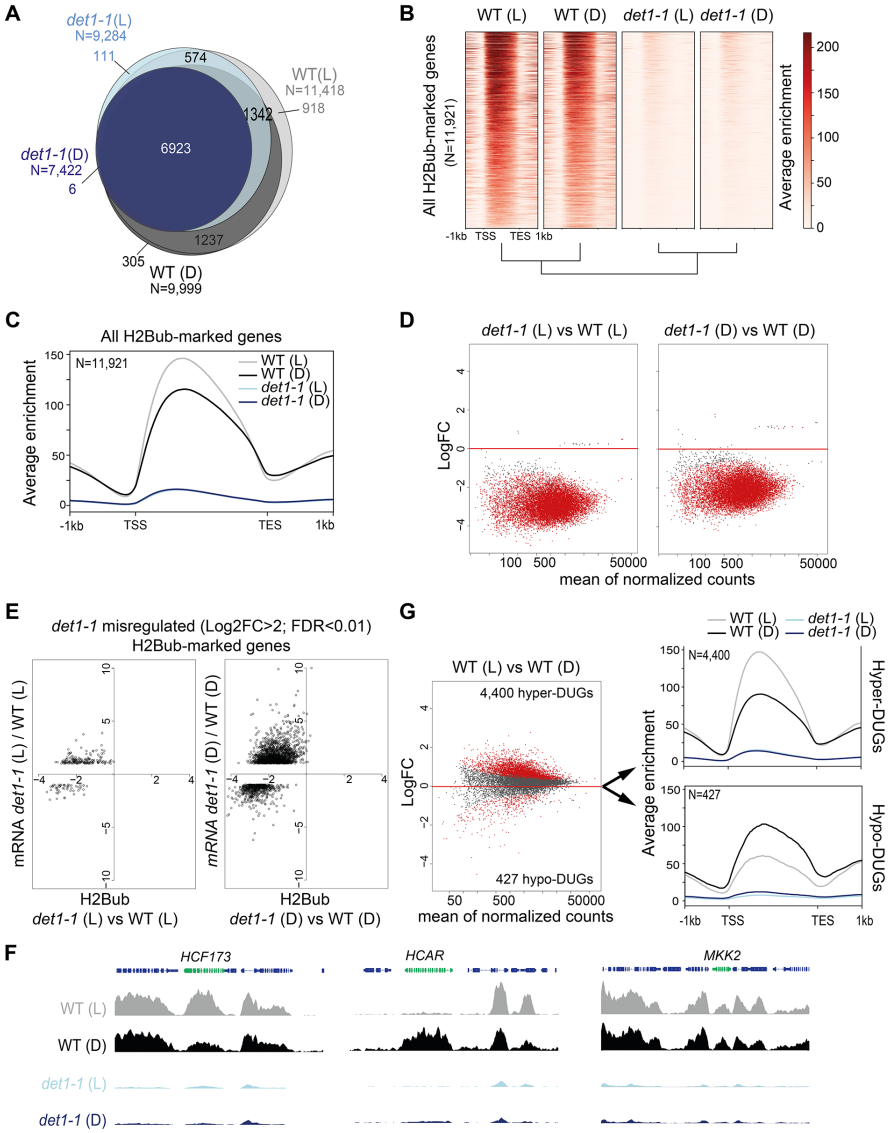

Figure 2. Light and DET1 massively influence H2Bub enrichment over protein-coding genes.

(A) Number of H2Bub-marked genes in 5-day-old wild-type (WT) and *det1-1* seedlings grown under light (L) or dark (D) conditions. A gene was considered as being marked when overlapping a H2Bub peak in each of the two biological replicates. **(B)** Heatmap showing dramatically low H2Bub levels over H2Bub-marked genes in *det1-1* seedlings. Genes are ranked from top to down according to H2Bub level in the WT (L) sample. **(C)** Metagene plot of H2Bub distribution over the coding regions of the 11,921 H2Bub-marked genes in the four sample types. **(D)** Identification of differentially ubiquitinated genes (DUGs) by Rx-normalized DESeq2 analysis (FDR<0.01) shows that *det1-1* mutation triggers low H2Bub levels over almost all genes. Dots represent the full set of genes displaying a H2Bub domain (according to MACS2 peak detection, see Methods) in at least one sample type. Red dots correspond to differentially ubiquitinated genes (DUGs; FDR<0.01). **(E)** In both dark and light conditions, massive misregulation of gene expression occurred in a globally hypo-ubiquitinated H2B landscape in *det1-1* plants. Scatter plots show the correspondence between H2Bub and gene expression changes between WT and *det1-1* plants on *det1-1* misregulated genes in light (left) and dark (right) conditions. The x-axis shows Log2 fold-changes (FC) of H2Bub levels as determined by Rx-normalized DESeq2 analysis (FDR<0.01). The y-axis shows expression Log2 fold changes of as determined by DESeq2 (>2-fold variation, FDR<0.01). Only genes bearing a significant H2Bub domain according to MACS2 peak detection are shown. **(F)** Similar analyses as in (C) and (D) showing a tendency towards higher H2Bub enrichment in light than in dark condition in wild-type plants. The 4,400 hyper-DUGs and 427 hypo-DUGs in WT (L) versus WT (D) samples and their corresponding H2Bub meta-profile are shown. **(G)** Genome-browser snapshots showing H2Bub profiles in WT and *det1-1* seedlings grown in light or dark conditions. *MKK2* is invariably expressed and marked by H2Bub under dark and light conditions. *HCF173* is a hyper-DUG gene (Log2FC=1.3) induced by light (Log2FC=3.7) that was previously shown to require HUB activity for optimal inducibility by light (Bourbousse et al., 2012). In contrast, *HCAR* is a hypo-DUG (Log2FC=-3.4) repressed by light levels (Log2FC=-0.7). In (C) to (G) H2Bub levels were scaled according to ChIP-Rx normalization factors calculated for each sample type to adjust for quantitative IP/Input variations in H2Bub enrichment over the genome. In all analyses, each sample type is the mean of two independent biological replicates.

As previously reported (Schroeder et al., 2002), RNA-seq analyses performed on the same samples showed that *det1-1* mutation has a broad effect on gene expression, to a large extent mimicking the effect of light signals on the transcriptome in dark conditions (Figure S2A). In both dark and light conditions, gene expression misregulation occurred in a globally hypo-ubiquitinated H2B landscape in *det1-1* plants (Figure 2E). Small variations in H2Bub levels between dark and light-grown samples correlating with transcript levels could be detected in *det1-1* plants, although to a much lower extent than in wild-type plants (Figure S2B). All together, these observations indicate that DET1 impacts the whole H2Bub landscape, without apparent gene specificity and without clear functional impact on steady state transcript profiles.

Light triggers an increase of H2Bub enrichment over many genes

In line with the role of H2Bub in the induction of light-responsive genes (Bourbousse et al., 2012), variations in H2Bub levels between dark and light-grown plants correlating with transcript levels could be detected in WT plants (Figure S2B), as exemplified in Figure 2F for the two representative light-regulated genes *HCF173* and *HCAR* with opposite responsiveness to light. More unexpectedly, comparison of light- and dark-grown WT plants further unveiled a tendency for higher H2Bub chromatin enrichment in the light than in the dark condition. As compared to the dark condition, in the light i) the number of H2Bub-marked genes was 12% higher (Figure 2A), ii) H2Bub average enrichment was higher in meta-plots representing all 11,921 H2Bub-marked genes (Figure 2C) and accordingly, iii) genes hyper-ubiquitinated in the light (hyper-DUGs) were 10 times more numerous than hypo-DUGs (Figure 2G). Correlation analysis of read counts in all replicates confirmed a dual effect of both light and *det1-1* mutation on global H2Bub dynamics between dark and light conditions (Figure S2C).

Comparison of relative transcript levels in dark- and light-grown WT seedlings showed that an equivalent number of genes are up- and down-regulated by light (Figure S2A), with similar amplitude in transcript level variations (Figure S2D).Consequently, on their own, relative changes in gene expression do not seem to explain the global tendency for higher H2Bub enrichment in the light *versus* dark condition. Considering its genome-wide property, the process might relate to variations in H2Bub homeostasis. These findings unveil that H2Bub is globally more abundant on genes in photomophogenic than in etiolated seedlings, a light-driven dynamic that is lost upon *DET1* loss-of-function.

DDA1 associates with SGF11, a potential SAGA-like H2Bub de-ubiquitination component

Considering its implication in the ubiquitination pathway (Chory, 2010; Lau and Deng, 2012), we suspected that DET1 might exert a direct regulatory role on H2B ubiquitination. Attempts to detect physical interactions of either DET1 or of its tightly associated DDB1 adaptor protein with HUB1 or HUB2 by yeast-two-hybrid (Y2H) and by co-purification were unsuccessful (data not shown).

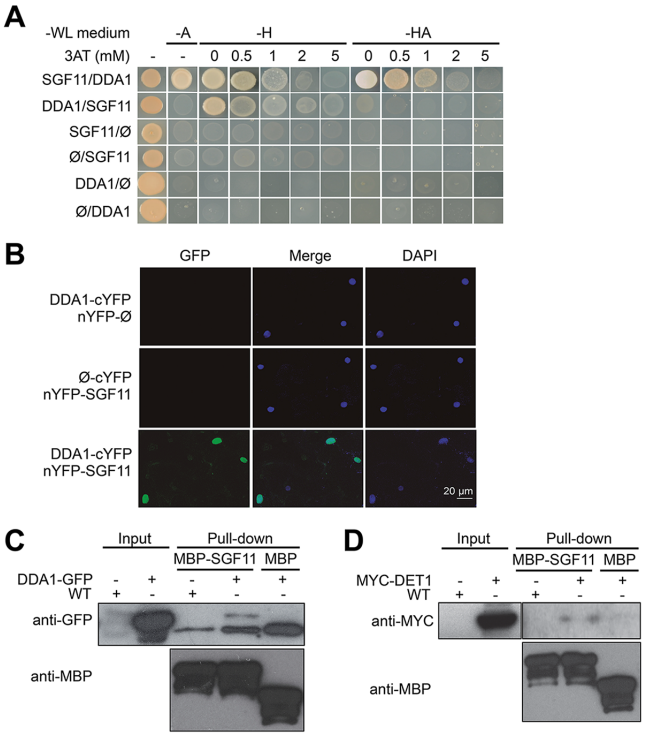

Figure 3. DDA1 C3D subunit physically associates with SGF11.
(A) Yeast-two-hybrid validation of DDA1-SFG11 interaction identified by Y2H screen. **(B)** BiFC analysis of DDA1 physical interaction with SGF11 *in planta*. Live fluorescence imaging 72h after dual transfection of Nicotiana leaves by plasmids expressing the indicated translational fusions. Merged images of GFP (left) and DAPI (right) channels are shown (middle). **(C-D)** DDA1 and DET1 associate with the SGF11 in plant extracts. Pull-down assays were performed using total protein extracts prepared from 7-d-old seedlings co-expressing DDA1-GFP (C) or MYC-DET1 (D) protein fusions with MBP-SGF11. Total extracts used (Input) and pull-down proteins were subjected to immunoblot analysis with anti-GFP, anti-MY and anti-MBP to detect the corresponding fusion proteins.

However, a Y2H screen using DDA1 as bait reproducibly detected the coding sequence of *AT5G58575*, a gene recently identified as the closest Arabidopsis ortholog of yeast *Sgf11* (Moraga and Aquea, 2015; Srivastava et al., 2015). *AT5G58575*, hereafter referred to as *SGF11*, encodes a protein with 31% and 19% sequence similarity with the SAGA DUB module component Sgf11/ATXN7L3 from *S. cerevisiae* and human, respectively (Figure S3). Reciprocal Y2H assays using a 3AT chase control confirmed the specific association of DDA1 with SGF11 (Figure 3A).

Bimolecular fluorescence complementation (BiFC) assays in *Nicotiana benthamiana* leaves further showed that SGF11 associates with DDA1 in plant nuclei (Figure 3B) but neither with DET1 nor with the other two C3D components COP10 and DDB1a (Figure S4). Finally, DDA1 and SGF11 were found to associate in Arabidopsis extracts using semi-*in vivo* maltose-binding protein (MBP) fusion pull-down assays (Figure 3C). Similar MBP assays showed that DET1 and SGF11 are also associated, although with a lower efficiency (Figure 3D). We conclude from these analyses that DDA1 physically associates with SGF11, a link that potentially allows bridging the C3D complex to a SAGA-like H2Bub deubiquitination activity.

SGF11 makes part of a trimeric H2Bub DUB module

Given the lack of knowledge on SAGA DUBm composition, structure and activity in the plant kingdom, we carried out Tandem Affinity Purification (TAP) analysis of SGF11 constitutively expressed in Arabidopsis cell cultures grown under either light or dark conditions (Figure 4A). This consistently identified peptides from four proteins in addition to SGF11 itself: two cytosolic TONNEAU1A/B proteins (Traas et al., 1987) as well as AT3G27100 and AT5G10790, two orthologous proteins of the yeast/Drosophila and human DUBm subunits SUS1/ENY2 and UBP22/USP22 proteins, respectively. SUS1 already referring to SUSPENSOR-1 in Arabidopsis (www.tair.org), these were named ENY2 and UBP22. Reciprocal TAP analyses using UBP22 as bait identified only SGF11 and ENY2, thus confirming robust co-purification of these three proteins (Figure 4A). Altogether, our TAP analyses allowed the co-purification of three of the four known SAGA DUBm subunits, and with SGF73 being conspicuously absent. Noteworthy, the Arabidopsis genome apparently encodes no orthologous genes of the yeast/human SGF73/ATXN7 (Moraga and Aquea, 2015; Srivastava et al., 2015), a subunit that is required for stabilizing and bridging DUBm to SAGA in other species (Durand et al., 2014). Our attempts to identify proteins displaying partial or full-length similarities to *S. cerevisiae* SGF73 primary or secondary structure in the genomes of green plant and algal lineages have also been unsuccessful (see Experimental Procedures).

Y2H and BiFC experiments were conducted to assess the mode of association between SGF11, ENY2 and UBP22. As observed in *S. cerevisiae* (Kohler et al., 2006), both analyses showed robust interactions of SGF11 with ENY2 and UBP22, but not between ENY2 and UBP22 (Figures 4B-C). To access how SGF11 might bridge ENY2 to UBP22 in the absence of an SGF73/ATXN7 ortholog, we modeled the tri-dimensional structure of the Arabidopsis DUBm based on their sequence homology with proteins of known structure. The best confidence model displayed high similarity to the yeast DUBm X-ray structure made of the four Sgf11, Ubp8, Sus1 and Sgf73 proteins (Samara et al., 2010) (Figure 4D). This representation shows conservation of the UBP22 Zn-finger domains positioning, in particular that potentially forming the conserved assembly lobe by encapsulating the long SGF11 amino-terminal α-helix with the central part of the small ENY2 protein (Kohler et al., 2010; Samara et al., 2010). The small ENY2 protein forms an interface between the UBP22 C-terminal domain and the long SGF11 α-helix, which may re-enforce the pairwise protein interactions in the DUBm (Figure 4C). A catalytic lobe oriented away from the assembly lobe can also be formed by the predicted ubiquitin-protease domain of UBP22. SGF11 C-terminal zinc-finger potentially allows interaction with a nucleosome and the ubiquitin moiety of H2Bub as shown in other species (Durand et al., 2014; Samara et al., 2012). Interestingly, long plant-specific amino- and carboxy-terminal extensions may protrude out from the conserved structural domains, possibly linking this core structure to other proteins or replacing the SAGA bridging-function of Sgf73.

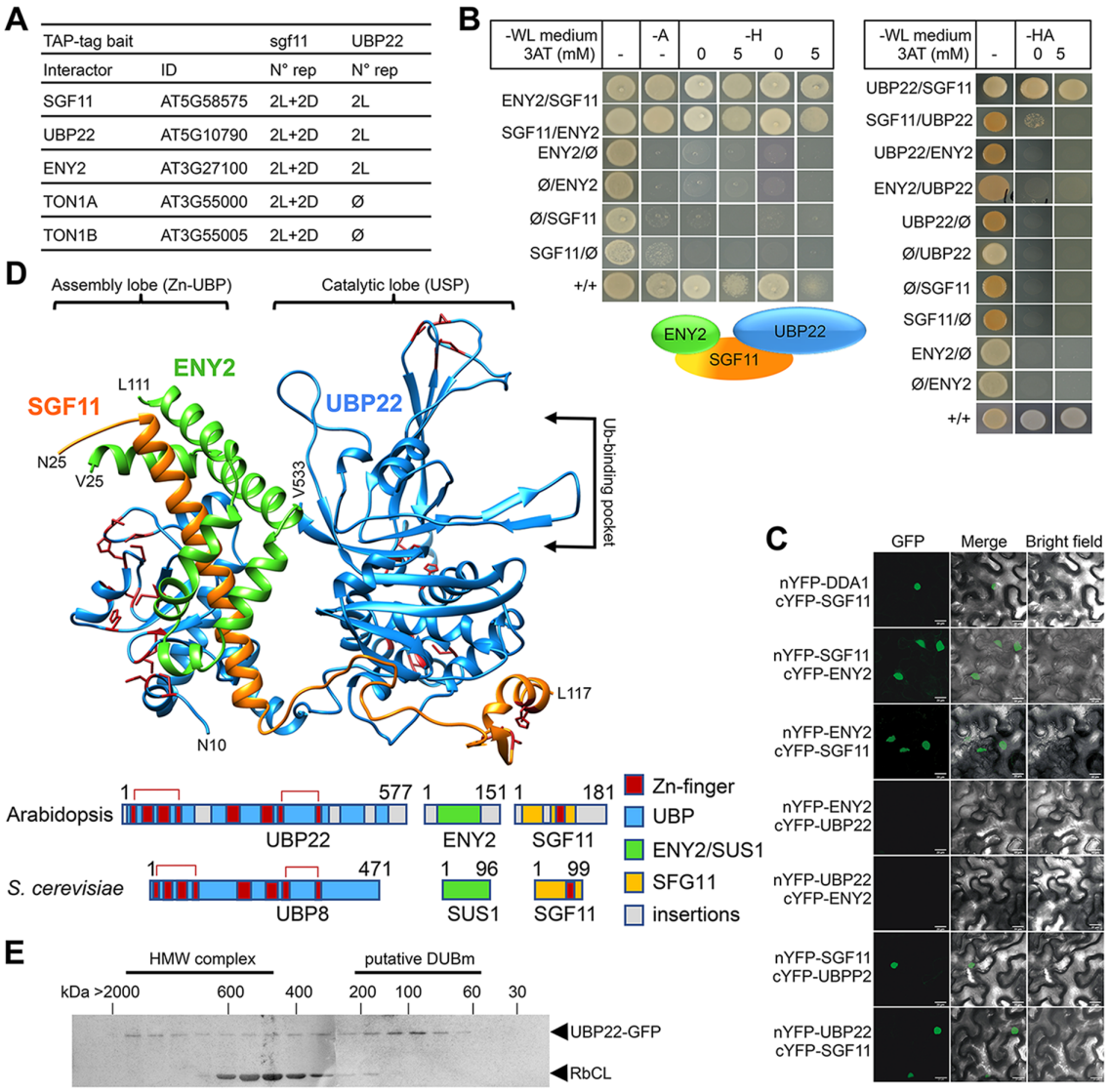

Figure 4. SGF11 physically associates with ENY2 and UBP22 to form an Ubp8-like DUBm. (A) TAP identification of UBP22 and ENY2 as SGF11-associated proteins. The table summarizes the whole set of detected proteins in each assay, including two independent replicates of dark (D) or light (L) grown cells using SGF11 as bait, and two independent biological replicates of light-grown cells when using UBP22 as a bait. **(B)** Yeast two-hybrid analysis of physical association between SGF11, UBP22 and ENY2 showing dual association of SGF11 with the two other DUBm components. **(C)** BiFC analysis of SGF11 interaction with UBP22 and ENY2 *in planta*. Merged images of GFP (left) and bright field (right) channels are shown (middle). **(D)** Top, modeled structure of the *Arabidopsis* UBP22-SGF11-ENY2 complex. Bottom, representation of domain similarities in the Arabidopsis and *S. cerevisiae* proteins (colored as indicated, gray areas reveal insertions that could not be modeled). The position of predicted Zn-finger domains in UBP22 and SGF11 is indicated in dark red in both panels. **(E)** Size-exclusion chromatography analysis of UBP22-GFP complex size in protein extracts from *UBP22::UBP22-GFP* Arabidopsis seedlings. Fractions were analyzed by anti-GFP immunoblot. The size of molecular-weight standard eluted in the same conditions is shown.

Arabidopsis transgenic lines stably expressing GFP-tagged SGF11, ENY2 or UBP22 were generated and used to investigate their subcellular localization, confirming that all proteins are nuclear-localized (Figure S5A). In agreement with the conserved function of SAGA in RNA Pol II transcription regulation, confocal imaging after anti-GFP immunolabeling further showed that SGF11 and UBP22 displayed punctuated signals in the euchromatin and are visibly excluded from densely DAPI-stained heterochromatic chromocenters and from the nucleolus. Euchromatic localization was also observed for DDA1-GFP and MYC-DET1 proteins (Figure S5B). By contrast, GFP-ENY2 signals were reproducibly enriched both in the euchromatic and heterochromatic compartments, sometimes overlapping with nucleolus-associated chromocenters (Figure S5B). Arabidopsis ENY2 might therefore display another activity independently from SGF11 and UBP22 in Arabidopsis, and may also differ

from its metazoan counterparts that are enriched at the nuclear periphery (Rodriguez-Navarro et al., 2004).

Taken together, these observations demonstrate that Arabidopsis SGF11, ENY2 and UBP22 associate *in planta* and potentially form a trimeric DUB module in the absence of an Sgf73/ATXN7 ortholog. To assess the stable accumulation of such a complex, a size-exclusion chromatography analysis of soluble protein fractions from the *UBP22::UBP22-GFP* plant line was performed. The ~100 kDa GFP-UBP22 protein was largely part of a 100-150 kDa complex, a size compatible with a tripartite association with the 20 kDa SGF11 and 13 kDa ENY2 proteins (Figure 4E). UBP22-GFP could also be detected (albeit to a much lower extent) in higher molecular weight fractions, which could correspond to SAGA-like complex size.

UBP22 is a major H2Bub deubiquitinase

To determine whether UBP22 displays H2Bub deubiquitination activity, we conducted a complementation assay of an *S. cerevisiae* Ubp8 knockout strain, a loss-of-function that induces aberrantly high H2Bub levels (Gardner et al., 2005; Henry et al., 2003). Expression of the full-length *UBP22* coding sequence under the control of the yeast *CYC1* promoter successfully restored normal H2Bub levels in independently transformed colonies (Figure 5A). UBP22 can therefore replace Ubp8 activity for H2Bub hydrolysis in the context of a *bona fide* SAGA complex.

To further test the influence of the Arabidopsis DUBm on H2Bub in plants, we obtained T-DNA insertion lines for *UBP22* and *SGF11*, hereafter referred to as *ubp22-1*, *sgf11-1* and *sgf11-2*. All homozygous plant lines were viable and displayed no obvious developmental phenotypes under standard laboratory growth conditions (Figure S6A). Immunoblot analyses showed a robust increase of H2Bub levels in each of these loss-of-function lines as compared to their wild-type counterparts, resulting in almost 50% of the histone H2B pool being monoubiquitinated instead of about ~15% in wild-type plants (Figure 5B-C). Re-introduction of a *UBP22* or *SGF11* functional coding sequence successfully restored low H2Bub levels in *ubp22-1* and *sgf11-1* plants, respectively (Figure S6B). As shown in Figure 5B, comparison with the previously identified histone H2Bub deubiquitination mutant line *ubp26-2* showed a more pronounced effect in *ubp22-1* (Sridhar et al, 2007). These observations indicate that UBP22 constitutes a major determinant of histone H2Bub deubiquitination and is necessary to maintain normal levels of H2Bub in Arabidopsis.

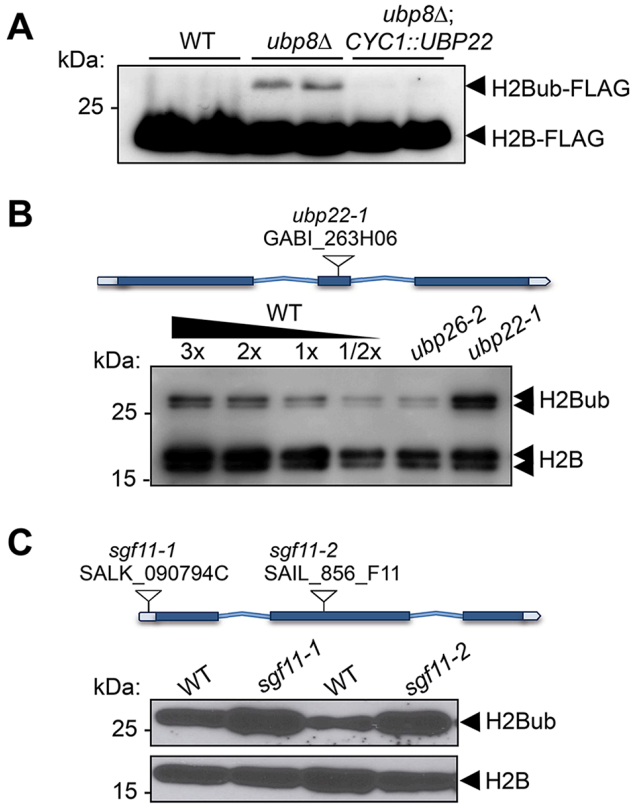

Figure 5. UBP22 is a functional homolog of the *S. cerevisiae* Ubp8 required for histone H2B deubiquitination in Arabidopsis. **(A)** Complementation of a *S. cerevisiae ubp8Δ* mutant line (Henry et al. 2003) by expression of the Arabidopsis *UBP22* CDS under the *Cyc1* promoter. For each line, FLAG-tagged histone H2B was detected by immunoblot analysis of whole cell extracts from two different yeast transformed colonies. **(B)** Anti-H2B immunoblot analyses of H2Bub in *ubp22-1* and *ubp26-2* mutant seedlings indicate that UBP22 has a more prevalent role than UBP26 in H2Bub removal. Core histone H2B (18kDa) forms and a doublet corresponding to monoubiquitinated H2B forms (~26 kDa) are detected in chromatin-enriched wild-type extracts. **(C)** Similarly to *ubp22-1*, *SGF11* loss of function triggers a large increase in H2Bub level. In (B) and (C), the position and ID of the different T-DNAs are depicted on the gene models.

Light and DET1 control the proteolytic degradation of the SGF11 DUBm subunit

Considering the dual effects of light and of *DET1* loss-of-function on H2Bub levels on one hand, and the physical association of DDA1 with the DUBm component SGF11 on the other, we tested whether SGF11 protein abundance was influenced by light conditions. Analysis of GFP-SGF11 expressed under the control of a 35S promoter (*35S::GFP-SGF11* plants) indeed showed lower levels in protein extracts from dark-grown than in light-grown seedlings (Figure 6A).

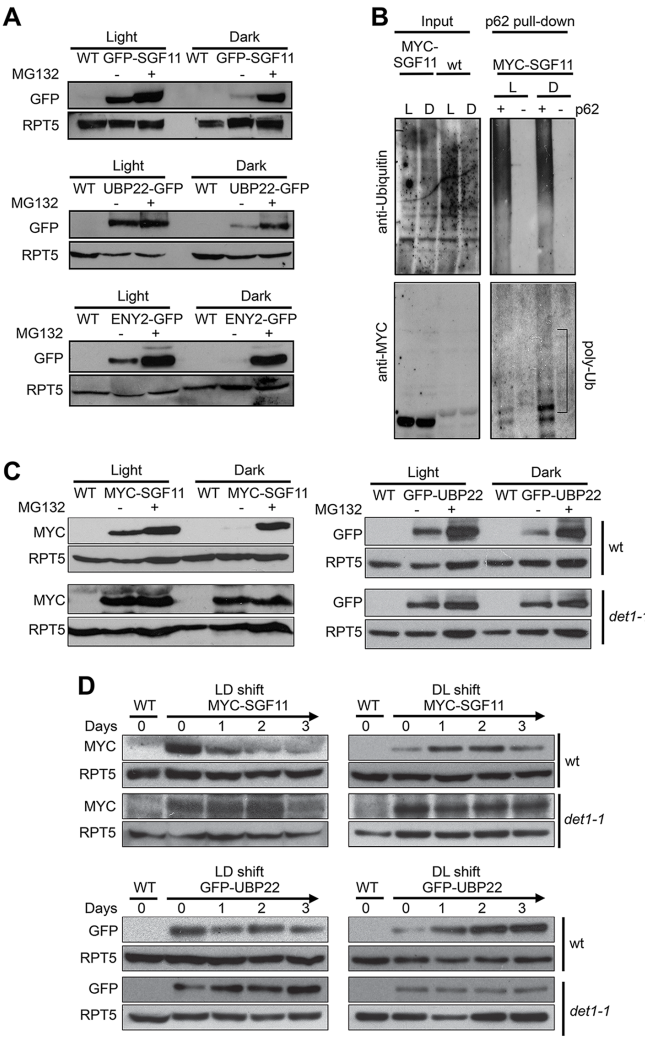

Figure 6. Light signaling controls the proteolytic degradation of the UBP22, SGF11 and ENY2 DUBm subunits. (A) UBP22, SGF11 and ENY2 DUBm components are degraded by the proteasome preferentially in darkness. Immunoblot analysis of GFP-tagged DUBm proteins in seedlings grown under continuous light or dark conditions. Prior to plant harvesting, seedlings were treated (+) or not (-) with 50 µM MG132 for 12h. **(B)** SGF11 is poly-ubiquitinated *in vivo*. MYC-SGF11 protein extracts from light (L)- and dark (D)-grown seedlings, treated (+) or not (-) with 50 µM MG132 for 12h, were incubated with p62 resin or with agarose resin as negative control. Ubiquitinated proteins are detected using anti-Ubiquitin antibody. Anti-MYC allows detection of MYC-SGF11 and its polyubiquitinated isoforms. Polyubiquitinated MYC-SGF11 signals are indicated (poly-Ub). **(C)** DET1 promotes the degradation of SGF11 and UBP22 preferentially in darkness. Analysis of the abundance of MYC-SGF11 and GFP-UBP22 proteins in wild-type and *det1-1* seedlings grown under dark or light conditions. Prior to plant harvesting, seedlings were treated (+) or not (-) with 50 µM MG132 for 12h. **(D)** DET1 promotes UBP22 and SGF11 protein degradation upon a light-to-dark shift. In (A-D), immunoblots were performed on whole-cell protein extracts from seedlings grown under the indicated conditions.

Pre-incubation of the plants with the MG132 proteasome inhibitor largely increased GFP-SGF11 accumulation to similar levels in both conditions. Similar effects were observed for the ENY2 and UBP22 proteins (Figure 6A), showing that abundance of all DUBm subunits is tightly controlled. Affinity purification of protein extracts from *35S::MYC-SGF11* seedlings with a ubiquitin-affinity resin showed that SGF11 proteins are poly-ubiquitinated under both dark and light conditions, with a more pronounced effect in darkness (Figure 6B). We concluded that stability of SGF11 is controlled by a proteasomal activity with a more prevalent effect in darkness.

Given the established role of the C3D complex in promoting protein degradation in darkness, we further tested whether the effect of light on SGF11 stability is mediated by DET1 after introgression of the *det1-1* allele in the *35S::MYC-SGF11* and *35S::GFP-UBP22* transgenic lines. Levels of both MYC-SGF11 and GFP-UBP22 were higher in *det1-1* than in wild-type plants in both conditions, indicating that DET1 is indeed required for SGF11 and UBP22 proteolytic degradation (Figure 6C).

To test for a dynamic regulation of SGF11 and UBP22 stability by light signaling, the *35S::MYC-SGF11* and *35S::GFP-UBP22* transgenic lines were submitted to dark-to-light and light-to-dark switches. Steady-state levels of the constitutively expressed recombinant MYC-SGF11 and GFP-UBP22 proteins exhibited dramatic changes during the transitions, which were already visible after 24 hours upon the transitions (Figure 6D, top panels). Furthermore, these changes were robustly dampened in the *det1-1* genetic background (Figure 6D, bottom panels). Taken together, these observations indicate that stability of the DUBm complex is regulated by the light signaling factor DET1.

DET1 antagonizes DUBm activity on H2Bub removal

Our findings point towards a model in which DET1 influences H2Bub homeostasis by opposing DUBm activity. To examine this possible antagonistic influence, we crossed the *det1-1* and *ubp22-1* lines and probed global H2Bub levels in double mutant plants. Immunoblot analyses indeed showed increased H2Bub levels in *det1-1ubp22-1* as compared to *det1-1* single mutant seedlings. Hence, loss of H2Bub triggered by *det1-1* is largely suppressed in the absence of a functional DUBm (Figure 7A and 7B).

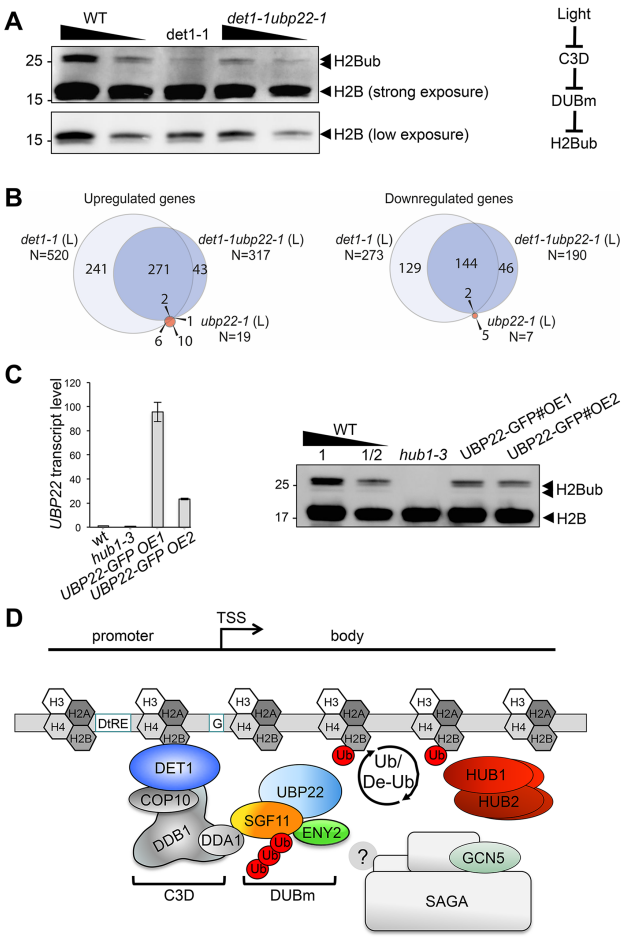

Figure 7. DET1 controls histone H2B monoubiquitination levels by opposing DUBm activity. (A) *UBP22* loss of function largely suppresses the loss of H2Bub in *det1-1* seedlings. Histone H2B (18kDa) and its monoubiquitinated H2B (~26 kDa) forms are detected with an anti-H2B antibody in immunoblot analysis of chromatin extracts from seedlings with the indicated genotypes. A scheme for the regulatory effects of light, C3D and DUBm on H2B ubiquitination homeostasis is depicted. **(B)** RNA-seq analysis of light-grown seedlings show that *det1-1* defects in gene expression are partially suppressed after introgression of the *ubp22-1* mutation, while *UBP22* loss-of-function *per se* only marginally affects gene expression in wild-type plants. The number of genes correspond to a Log2FC > 1 and a FDR < 0.01. **(C)** *UBP22* overexpression decreases histone H2Bub global level. Left panel, RT-qPCR measurement of *UBP22* transcript levels in overexpression lines #OE1 and #OE2 relative to the wild-type level (arbitrarily set to 1). Right panel, immunodetection of H2Bub levels in chromatin extracts from light-grown seedlings of the indicated genotypes. **(D)** Proposed model depicting the C3D complex activity in regulating histone H2Bub homeostasis through ubiquitin-mediated control of the DUBm stability. UBP22 is a Ubp8 homolog acting with SGF11 and ENY2 in H2Bub deubiquitination, possibly promoting transcription under optimal growth conditions. The C3D complex DDA1 subunit targets SGF11 for degradation, favoring degradation of the DUBm. DET1 affinity for non-acetylated histone H2B (Benvenuto et al, 2002) may favor this degradation nearby H2Bub-rich regions. DET1 may further influence histone H2B acetylation status via an unknown mechanism, possibly involving the DUBm/SAGA activities or independent pathways. In the absence of *Sgf73* homolog in plants, the DUBm may act independently from SAGA.

To provide a more functional assessment on the antagonistic activities of DET1 and DUBm, we determined the transcriptome profile of *det1-1ubp22-1* seedlings and compared it with those of WT, *det1-1* and *ubp22-1* plants (Figure 7B). As reported for the yeast *ubp8Δ* strain (Gardner et al., 2005; Lenstra et al., 2011), differential analyses of gene expression showed that *UBP22* loss-of-function only marginally affects transcript levels - with just 26 genes being misregulated in *ubp22-1* as compared to WT plants (Figure 7B). Secondly, in line with the former hypothesis, *det1-1ubp22-1* double mutant plants displayed a partially suppressed transcriptome phenotype, the expression of about half (53%) of the *det1-1* up- or downregulated genes being restored after simultaneous *UBP22* loss-of-function (Figure 7B).

Our results also predict that over-accumulation of the DUBm in *det1-1* plants is responsible, at least partially, for the reduction of H2Bub levels in this mutant. The generation of independent transgenic lines in which *UBP22-GFP* is overexpressed (*wt/UBP22-GFP#OE1 and #OE2*) indeed confirm that UBP22 is a limiting factor in H2Bub removal (Figure 7C). Taken together, these findings indicate that DET1-mediated control of DUBm proteolytic degradation represents a previously unidentified mechanism to adjust H2Bub levels, which can mediate light-dependent control on H2Bub homeostasis over the genome.

Discussion

Photomorphogenesis combines drastic changes of chromatin organization, transcriptional activity and H2Bub enrichment over the genome

Many plant cells are subjected to drastic transcriptomic and metabolic changes during the photomorphogenic transition, a process also involving nuclear expansion, heterochromatin condensation, and variations of nucleosomal accessibility over a large repertoire of genes (Bourbousse et al., 2015; Peschke and Kretsch, 2011; Sullivan et al., 2014). Hundreds of genes are differentially marked by H2Bub during de-etiolation, a phenomenon that we could link to co-occurring gene expression changes (Bourbousse et al., 2012), many of which undergo pioneering rounds of transcription during photomorphogenesis (reviewed in (Barneche et al., 2014; Perrella and Kaiserli, 2016). Accordingly, dual detection of non-phosphorylated

and Ser-5 phosphorylated RNA Pol II CTD in individual cotyledon nuclei has shown that the proportion of RNA Polymerase II molecules engaged in transcription increases more than twice when comparing dark and light conditions (Bourbousse et al., 2015). The H2Bub ChIP-Rx analysis performed here further reveals that H2Bub abundance is globally controlled during photomorphogenesis. H2Bub levels were significantly higher on many H2Bub-marked genes in the light than in the dark, while only a few genes, usually light-repressed, display an opposite tendency. This extra layer of information unveils the existence of a control on H2Bub homeostasis by light signaling. Interestingly, the SAGA DUBm mediates the regulation of genes involved in axon targeting and neuronal connectivity in the Drosophila visual system (Weake et al., 2008), indicating that functional links between H2Bub deubiquitination and light-related functions exist in distant eukaryotic species.

We further report that the photomorphogenesis regulator DET1 is required for shaping the H2Bub landscape. *DET1* loss-of-function triggers a decrease of H2Bub level throughout almost all genes, a defect that we found to be genetically linked to *UBP22* function. This protein was found to be part of an atypical SAGA-like DUB module whose abundance is regulated by DET1 during dark/light transitions. Taken together, these observations indicate that an active mechanism regulates the availability of the Arabidopsis DUBm, in which DET1 is directly involved. Indeed, SGF11 was found to physically associate with the C3D component DDA1 in two-hybrid experiments and *in planta*. SGF11 is subjected to DET1-dependent poly-ubiquitination and proteolytic degradation, with a more pronounced effect in the dark. Stability, and hence cellular availability of Arabidopsis DUBm is directly controlled by light signaling.

Our observation of coincidentally low levels of DUB subunits and of H2Bub over the genome in dark condition appears counter-intuitive. Dampening of these two antagonistic components also appear to match a partially poised transcriptional status of fully etiolated seedling cells, a property that might be linked in this case to their stalled development. Although causal relationships cannot be established at this stage, our observations point towards a concerted light-triggered reprogramming of H2Bub homeostasis and cellular transcriptional activity in this biological system. Indeed, RNA Pol II elongation constitutes an essential regulatory step of productive transcription (reviewed in (Li et al., 2007; Selth et al., 2010; Weake and Workman, 2008) and histone H2B monoubiquitination is intimately linked with global transcriptional elongation capacity in mammalian cells (Minsky et al., 2008). Our observations provide a first potential mechanism as to how the cell controls H2Bub homeostasis during cell specialization. Determining whether modulation of H2Bub levels during photomorphogenesis primarily influences a cell's capacity for transcription elongation or other processes such as DNA replication or cell cycle progression will require additional investigation.

An atypical H2Bub DUB module is targeted by light signaling for ubiquitin-mediated proteolysis

Despite their involvement in basal cellular mechanisms, RNA Pol II-associated chromatin machineries must themselves be controlled to influence the transcriptional capacity. In budding yeast, the proteasomal ATPase Rpt2 interacts with Sgf73 to dissociate the DUBm from SAGA (Lim et al., 2013). Being apparently absent from their genome, a *Sgf73*-based regulatory mechanism cannot be at play in plants. Our data rather unveil a control of the DUBm abundance through targeted proteolysis of the SGF11 subunit. Similar to the SAGA DUBm structure in yeast (Kohler et al., 2006), we found that Arabidopsis SGF11 associates with UBP22 and ENY2, and accordingly is centrally positioned in the modeled UBP22 DUBm structure. Hence, SGF11 proteolytic degradation is expected to efficiently impair the DUBm activity. UBP22 and ENY2 degradation could either be an indirect consequence of SGF11 proteolysis, or result from a C3D-dependent targeted degradation of the other two subunits. Like for many other protein complexes structured by pair-wise interactions, elimination of *Ubp8*, *Sgf11* or S*us1* induces a loss of the other members of the DUBm in yeast, and the same might occur in Arabidopsis. This possibility is supported by the observation that reconstitution of the yeast tetrameric DUBm *in vitro* requires co-expression of Sus1 and Sgf11 (reviewed in (Rodriguez-Navarro, 2009).

Given that SGF73/ATXN7 is required for bridging the DUBm to the SAGA core domain in yeast and human (Kohler et al., 2008; Lee et al., 2005; Lee et al., 2009), identification of a functional SAGA-like DUBm in Arabidopsis lacking a potential ortholog raises questions about the complex formation and activity in plants. Size-exclusion chromatography suggests that UBP22 may to some extent accumulate as a high-molecular weight complex. In contrast, our multiple TAP analyses were unsuccessful in

identifying other SAGA components. Some functional independency between the DUBm and other SAGA modules has been proposed in other species, with the capacity of a trimeric Ubp8–Sgf11–Sus1 complex to dissociate from SAGA (Kohler et al., 2006). The capacity of Arabidopsis ENY2-SGF11-UBP22 to form a fully functional module remains to be tested. Characterizing the function of SGF11 and ENY2 amino or carboxy-terminal extra-domains might reveal how functionality is achieved in a trimeric complex. This might also help to understand the relationship between SAGA-dependent histone acetylation activity and H2Bub dynamics during transcription initiation and elongation in plants. Our mass spectrometry and immunoblot analyses allowed the detection of multiple acetylation defects in histone H2B and H3 in *det1-1* plants. These might result from independent functions of the DET1 protein or possibly also from consequences of impaired SAGA activity. Defective histone acetylation in this mutant line could be meaningful given the influence of histone H2B acetylation for DET1 binding (Benvenuto et al., 2002). Hence, concerted action of SAGA HAT and DUBm activity might both impact DET1 affinity for histone H2B, possibly triggering dynamic changes in DET1 association with chromatin.

A direct role for DET1 on histone H2B

Despite having no detectable DNA binding capacity, DET1 can act as a potent transcriptional repressor acting in *cis* on light- and circadian-clock regulated genes in plants or when exogenously expressed in yeast cells (Lau et al., 2011; Maxwell et al., 2003). This property has been long proposed to relate to its association with histone H2B (Benvenuto et al., 2002) but thus far no mechanism has been identified. Here we uncover that DET1 is involved, presumably via the physical association of DDA1 with SGF11, in controlling abundance of a chromatin machinery linked to histone H2B and to RNA Pol II activity. In particular, we propose a possible mechanism involving recruitment of the DDA1 C3D subunit on genomic regions where DET1-mediated modulation of DUBm stability controls H2Bub chromatin enrichment (Figure 7D). Decreasing the DUBm availability in darkness might represent a way for the plant cell to trigger global changes in this chromatin mark, possibly dampening H2Bub turnover capacity in cells with a low transcriptional status.

This study shows how the availability of transcriptional co-activator machineries can be modulated by an environmental signal. The impact of Arabidopsis DET1 on the DUBm stability adds to the knowledge that CRL4 activities influence H2Bub dynamics, as shown in the context of circadian clock-controlled gene expression in mammals (Tamayo et al., 2015) and of DNA repair pathways in *Schizosaccharomyces pombe* and human cells (Martinez et al., 2001; Zeng et al., 2016). Our findings on plant photomorphogenesis echo situations in which metazoan cells are also subject to drastic changes in cell identity and proliferation. For example, misregulation of H2Bub homeostasis appears to be central in the transcriptional events linked to human oncogenesis, as *USP22* transcript abundance is part of an 11-gene signature that associates with poor cancer prognosis (Jeusset and McManus, 2017), hence potentially influencing cell proliferation processes like human DET1 (Pick et al., 2007; Wertz et al., 2004). Considering the evolutionary conservation of DET1, DDA1 and of the three plant DUBm components from plants to metazoans, future studies might unveil a functional link between DET1 activity and DUBm abundance in other organisms.

Methods and Materials

Plant lines and growth conditions

Seeds were surface-sterilized, plated on MS medium 0.9% agar without sugar and, unless stated otherwise, cultivated under either a 16h/8h (23/19°C) light/dark photoperiod (100 µmol.m^{-2}.s^{-1}) or constant (light/23°C or dark/23°C) conditions. Some samples were further exposed to white light (100 µmol.m^{-2}.s^{-1}) for the indicated duration and seedlings were harvested concomitantly at 4pm (8zt) under a green safe light for RNA or ChIP extractions. All plant lines are in the Columbia-0 ecotype background. The *det1-1* (Chory et al., 1989), *hub1-3* (GABI_276D08) (Fleury et al., 2007), *hub2-2* (SALK_071289)(Liu et al., 2007), *ubp26-2* (Sridhar et al., 2007), *35S::MYC-ubiquitin* (Dubin et al 2008) and 35S::MYC-DET1 (Castells et al., 2011) Arabidopsis lines have been previously described. The *ubp22-1* (GABI_263H06), *sgf11-1* (SALK_090794C) and *sgf11-2* (SAIL_856_F11) insertion lines were obtained from the NASC (Scholl et al., 2000). The generation of transgenic lines and oligonucleotide sequences are given in the Supplementary Experimental Procedures.

Plant protein extraction, MBP pull-down assays, TAP-tag purification and immunoblotting

Chromatin-enriched protein fractions were obtained as previously described (Bourbousse et al., 2012). Whole cell protein extracts were obtained by thawing grinded material in 1M Tris-HCl pH8, 20% SDS, 15% glycerol, cOmplete EDTA-free protease inhibitor cocktail (Sigma-Aldrich) followed by centrifugation two times 10 min 16,000 g at 4°C. Extraction of plant soluble protein extracts was performed in 50 mM Tris-HCl, pH 7.4, 150 mM NaCl, 10 mM MgCl2, 1 mM phenylmethylsulfonyl fluoride, 0.1% Nonidet P-40 and cOmplete EDTA-free protease inhibitor cocktail (Sigma-Aldrich) followed by centrifugation two times 10 min 16,000 g at 4°C. Protein concentration in the final supernatants was determined using the Bio-Rad Protein Assay kit. Boiled protein samples were separated by 8-14% SDS-PAGE, transferred on Immobilon-P membranes (Millipore) and blotted with the antibodies detailed in the Supplementary Information. Affinity purification of ubiquitinated proteins according to (Manzano et al., 2008) is described in the Supplementary Experimental Procedures. For pull-down assays, equal amounts of seedling protein extracts were combined with 6 µg of the indicated MBP-tagged fusion or MBP protein alone, bound to amylose resin for 1 h at 4°C with rotation, washed three times with 1 mL of extraction buffer, eluted and denatured in sample buffer before immunoblot analysis. TAP-tag analysis of SGF11 and UBP22 associated proteins was performed as described in (Van Leene et al., 2015). Protein interactors with at least two matched high confident peptides identified by mass spectrometry were retained. Background proteins were filtered out based on frequency of occurrence of the co-purified proteins in a large dataset (Van Leene et al., 2015). More detailed information on TAP and other protein analyses is given in the Supplementary Experimental Procedures.

Histone proteomics analyses

Histone proteins samples were prepared from 50 mg of plant material by preparing chromatin-enriched fractions following the ChIP protocol (omitting the formaldehyde crosslinking step) and subsequent purification of 1 mg proteins re-suspended in ChIP Nucleus Lysis Buffer (SDS 1%, EDTA 10mM, Tris pH8) using the Histone Purification Mini kit (Active Motif) following the manufacturer's instructions. All peptide/protein identification data were processed using the Institut Curie-developed software myProMS version 3 (Poullet et al., 2007) in which the false discovery rate for peptide identification was set to <0.01. More detailed information on histone processing, label-free quantification, and the identification of H2B monoubiquitinated residue is given in the Supplementary Material.

Cytological analyses

Immunolocalization of fixed proteins in isolated nuclei was performed on 7-days-old seedlings as described in (Bourbousse et al., 2015) using the antiboodies given in Supplementary Procedures. Images were acquired using a confocal laser-scanning microscope (SP5, Leica) and processed using ImageJ (rsb.info.nih.gov/ij/). For BiFC experiments, Agrobacterium strains expressing the indicated combinations of fusion proteins were co-infiltrated into the abaxial surface of 3-week-old *Nicotiana benthamiana* plants using the p19 protein to suppress gene silencing as described in (Irigoyen et al., 2014). Fluorescence was visualized in leaf epidermal cells 3 days after infiltration using a Leica SP5 confocal microscope.

Size-exclusion chromatography

Ten-day-old seedlings were ground in liquid nitrogen and resuspended in 1ml of extraction buffer (50mM Tris–HCl pH 7.5, 150mM NaCl, 5mM EDTA, 0.1% NP-40, 10% glycerol and protease inhibitors). The extract was cleared by successive centrifugation for 5min at 5,000 g, 5 min at 10,000 g and 1h at 16,000 g. The soluble fraction was subsequently concentrated at 14,000 rpm in YM-10 centricons (Amicon). About 250µL (1mg) of cleared extract was injected in a pre-calibrated Superdex 200 gel filtration column (GE Healthcare) and run with the same extraction buffer at 0.4 ml.min-1 in an AKTA FPLC system. Twenty 0.5 ml fractions were collected and analyzed by immunoblotting with an anti-GFP antibody (632381 Clontech).

Yeast experiments

For yeast complementation assays, the *UBP22* coding sequence was amplified using primers AT-NOT1-22 and 22-PSTI-AT adding a Not1 and a Pst1 restriction site in 5' and 3', respectively, of the CDS and ligated into a pCRII-TOPO vector. UBP22 Not1/Pst1 restriction products were further inserted in the pCM185 plasmid (ATCC 87659). The yeast strain *ubp8Δ* (UCC6392; (Gardner et al., 2005) was transformed by heat shock and total proteins from randomly spotted colonies were extracted using 8M urea SDS loading buffer to assess H2Bub levels by immunoblot. Primer sequences are given in

Supplementary Procedures. Yeast-two-hybrids experiments were performed using the Matchmaker™ (Clontech) system according to the manufacturer instructions. Both bait and prey empty vectors were used as negative controls.

Protein sequence analyses and modeling

The structure of UBP22, SGF11 and ENY2 were predicted using the Phyre2 web portal for protein modeling, prediction and analysis (http://www.sbg.bio.ic.ac.uk/phyre2/) (Kelley et al., 2015). The best models for AtUBP22 and AtSGF11 were based on the structure of ScUbp8 and ScSgf11 within the yeast DUBm at 1.89 Å resolution (PDB code 3MHS, (Samara et al., 2010) with 100 % confidence and 80 % sequence coverage, and 99.9 % confidence and 51 % sequence coverage, respectively. AtENY2 best model was based on the structure of ScSus1 within the yeast TREX-2 complex at 2.7 Å resolution (PDB code 3FWC) with 99.9 % confidence and 58 % sequence coverage. In the later case, a structural homology search using DALI (Holm and Laakso, 2016) recognizes ScSus1 in the DUBm context with a high score (Z-score = 10.2 with a rmsd of 2.1 Å over 85 residues). Protein visualization was done using UCSF Chimera (https://www.cgl.ucsf.edu/chimera). A potential SGF73 plant homolog was searched by identifying proteins displaying partial or full-length similarities to *S. cerevisiae* SGF73 primary structure from the 33,090 non-redundant protein sequence database of green plants and the 3,027 protein sequence database of algae (PSI-BLAST), or secondary structure from *Arabidopsis thaliana* (TAIR10) and *Chlamydomonas reihnardtii* (Jul_27_2017) proteomes (HHPRED; (Zimmermann et al., 2017).

ChIP-Rx experiments

ChIP experiments were conducted as described previously (Bourbousse et al., 2012) in two biological replicates of 5-day-old WT and *det1-1* seedling grown under light or constant dark conditions using an anti-H2Bub antibody (MM-0029-P, Medimabs). For each biological replicate, two IPs were carried out using 100µg of Arabidopsis chromatin mixed with 3µg of Drosophila chromatin, as quantified using BiCinchoninic acid Assay (Thermo Fisher Scientific). Eluted and purified DNA from the two technical replicates were pooled before library preparation (Illumina TruSeq ChIP) and sequencing (Illumina sequencing single-reads, 1x50bp) of the resulting 8 input and 8 IP samples by Fasteris (Geneva, Switzerland). Spike-in normalization was performed as described in (Orlando et al., 2014) with some modifications. Reads were mapped onto the Arabidopsis thaliana (TAIR10) and Drosophila melanogaster (dm6) genomes using STAR (Dobin et al., 2013). Drosophila-derived reads were first normalized according to the number of input reads in each sample and used to calculate a Rx scaling factor for each replicate. Rx factors were used to scale browser tracks (Thorvaldsdottir et al., 2013) and for DESeq2 detection of DUGs. See Supplemental Information for a more detailed description.

RNA analyses

For RT-qPCR experiments, 1 µg of total RNA was isolated with the NucleoSpin RNA Plant kit (Macherey Nagel), treated with Amplification Grade DNaseI (Invitrogen), and cDNAs were synthesized using the High-Capacity cDNA Reverse Transcription kit (Applied Biosystems). Quantitative PCR was carried out using the LightCycler 480 SYBR Green I Master (Roche). *UBP22* transcripts were quantified using the primer pair UBP22_RT1_Fwd and UBP22_RT1_Rev and results were normalized to *ACT2* transcript levels using ACTIN2_CF_F and ACTIN2_CF_R primers. For RNA-seq experiments, total RNAs from 5-day-old seedlings independently grown in two biological replicates were extracted using the Quick-RNA MiniPrep kit (Zymo) and processed independently. Library preparation and sequencing (Illumina sequencing single-reads, 1x50bp) was performed by Fasteris (Geneva, Switzerland) using 1µg of RNA. Reads were mapped onto the TAIR10 reference genome using STAR (Dobin et al., 2013). Detection of DEGs was performed on raw read counts using DESeq2 (Love et al., 2014) to obtain normalized fold change and FDR values for each gene. See Supplemental Information for a more detailed description.

Acknowledgements

The authors gratefully acknowledge Alexandre Sta (Institut Curie, Paris, France) and Magalie Charvin (IBENS, Paris, France) for statistical assistance, Jérome Deraze and Frédérique Perronet (Institut de Biologie Paris Seine, France) for providing Drosophila samples, Daniel E. Gottschling (Fred Hutchinson Cancer Research Center, USA) for providing the *ubp8Δ* yeast strain (Gardner et al., 2005) and Lionel Schiavolin for unpublished work (IBENS, Paris, France). They also thank Roberto Solano (CNB,

Madrid, France), Crisanto Gutiérrez (CBM Severo Ochoa, Madrid, Spain), Daniel Bouyer and Vincent Colot (IBENS, Paris, France) for helpful discussions. Work in ChB and FB laboratory was supported by grant ANR-11-JSV2-003-01 from the Agence Nationale pour la Recherche (ANR), the Investissements d'Avenir program launched by the French Government and implemented by ANR (ANR-10-LABX-54 MEMOLIFE and ANR-10-IDEX-0001-02 PSL* Research University), and a PhD fellowship from the Université Paris-Sud Doctoral School in Plant Sciences. Research in VR laboratory was supported by Grants BIO2013-46539-R and BIO2016-80551-R funded by MINECO and AEI/FEDER/EU. AN, EI and SF were supported by "Fundación La Caixa", MINECO FPI and "Ramón y Cajal" Program fellowships.

Author Contributions

All authors contributed reagents, materials or analysis tools. AN, MR, GZ, AFD, DS, SD and SF performed all protein analyses except TAP analyses that were carried out by EI, DE and GdJ. AN and SD performed DNA cloning. ClB conducted RNA-seq experiments. ClB and MR performed ChIP-seq experimental work. Bioinformatics analyses were conducted by OAM, IA and ClB. CéB performed protein sequence modeling. AN, MR performed microscopy analyses. VM and BL carried out histone MS experimental work; DL supervised histone MS data analysis. VR, ChB and FB conceived the experiments in close interaction with all their laboratory members, rose funding and wrote the manuscript. All authors read and approved the manuscript.

Competing interests

The authors declare that no competing interests exist.

References

Antosz, W., Pfab, A., Ehrnsberger, H.F., Holzinger, P., Kollen, K., Mortensen, S.A., Bruckmann, A., Schubert, T., Langst, G., Griesenbeck, J*., et al.* (2017). The Composition of the Arabidopsis RNA Polymerase II Transcript Elongation Complex Reveals the Interplay between Elongation and mRNA Processing Factors. The Plant cell *29*, 854-870.

Baptista, T., Grunberg, S., Minoungou, N., Koster, M.J.E., Timmers, H.T.M., Hahn, S., Devys, D., and Tora, L. (2017). SAGA Is a General Cofactor for RNA Polymerase II Transcription. Molecular cell *68*, 130-143 e135.

Barneche, F., Malapeira, J., and Mas, P. (2014). The impact of chromatin dynamics on plant light responses and circadian clock function. Journal of experimental botany *65*, 2895-2913.

Belotserkovskaya, R., Oh, S., Bondarenko, V.A., Orphanides, G., Studitsky, V.M., and Reinberg, D. (2003). FACT facilitates transcription-dependent nucleosome alteration. Science *301*, 1090-1093.

Benhamed, M., Bertrand, C., Servet, C., and Zhou, D.X. (2006). Arabidopsis GCN5, HD1, and TAF1/HAF2 interact to regulate histone acetylation required for light-responsive gene expression. Plant Cell *18*, 2893-2903.

Benvenuto, G., Formiggini, F., Laflamme, P., Malakhov, M., and Bowler, C. (2002). The photomorphogenesis regulator DET1 binds the amino-terminal tail of histone H2B in a nucleosome context. Curr Biol *12*, 1529-1534.

Bergmuller, E., Gehrig, P.M., and Gruissem, W. (2007). Characterization of post-translational modifications of histone H2B-variants isolated from Arabidopsis thaliana. J Proteome Res *6*, 3655-3668.

Berloco, M., Fanti, L., Breiling, A., Orlando, V., and Pimpinelli, S. (2001). The maternal effect gene, abnormal oocyte (abo), of Drosophila melanogaster encodes a specific negative regulator of histones. Proceedings of the National Academy of Sciences of the United States of America *98*, 12126-12131.

Bonnet, J., Wang, C.Y., Baptista, T., Vincent, S.D., Hsiao, W.C., Stierle, M., Kao, C.F., Tora, L., and Devys, D. (2014). The SAGA coactivator complex acts on the whole transcribed genome and is required for RNA polymerase II transcription. Genes & development *28*, 1999-2012.

Bourbousse, C., Ahmed, I., Roudier, F., Zabulon, G., Blondet, E., Balzergue, S., Colot, V., Bowler, C., and Barneche, F. (2012). Histone H2B monoubiquitination facilitates the rapid modulation of gene expression during Arabidopsis photomorphogenesis. PLoS Genet *8*, e1002825.

Bourbousse, C., Mestiri, I., Zabulon, G., Bourge, M., Formiggini, F., Koinig, M., Spencer C., B., Fransz, P., Bowler, C., and Barneche, F. (2015). Heterochromatin reorganization during photomorphogenic reprogramming of plant development. Proceedings of the National Academy of Sciences of the United States of America *112*, E2836-2844.

Cao, Y., Dai, Y., Cui, S., and Ma, L. (2008). Histone H2B monoubiquitination in the chromatin of FLOWERING LOCUS C regulates flowering time in Arabidopsis. Plant Cell *20*, 2586-2602.

Casal, J.J. (2013). Photoreceptor signaling networks in plant responses to shade. Annu Rev Plant Biol *64*, 403-427.

Castells, E., Molinier, J., Benvenuto, G., Bourbousse, C., Zabulon, G., Zalc, A., Cazzaniga, S., Genschik, P., Barneche, F., and Bowler, C. (2011). The conserved factor DE-ETIOLATED 1 cooperates with CUL4-DDB1DDB2 to maintain genome integrity upon UV stress. Embo J *30*, 1162-1172.

Charron, J.B., He, H., Elling, A.A., and Deng, X.W. (2009). Dynamic landscapes of four histone modifications during deetiolation in Arabidopsis. Plant Cell *21*, 3732-3748.

Chory, J. (2010). Light signal transduction: an infinite spectrum of possibilities. Plant J *61*, 982-991.

Chory, J., Peto, C., Feinbaum, R., Pratt, L., and Ausubel, F. (1989). Arabidopsis thaliana mutant that develops as a light-grown plant in the absence of light. Cell *58*, 991-999.

de Jonge, W.J., O'Duibhir, E., Lijnzaad, P., van Leenen, D., Groot Koerkamp, M.J., Kemmeren, P., and Holstege, F.C. (2017). Molecular mechanisms that distinguish TFIID housekeeping from regulatable SAGA promoters. The EMBO journal *36*, 274-290.

Dobin, A., Davis, C.A., Schlesinger, F., Drenkow, J., Zaleski, C., Jha, S., Batut, P., Chaisson, M., and Gingeras, T.R. (2013). STAR: ultrafast universal RNA-seq aligner. Bioinformatics *29*, 15-21.

Durand, A., Bonnet, J., Fournier, M., Chavant, V., and Schultz, P. (2014). Mapping the deubiquitination module within the SAGA complex. Structure *22*, 1553-1559.

Edgar, R., Domrachev, M., and Lash, A.E. (2002). Gene Expression Omnibus: NCBI gene expression and hybridization array data repository. Nucleic acids research *30*, 207-210.

Feng, J., and Shen, W.H. (2014). Dynamic regulation and function of histone monoubiquitination in plants. Frontiers in plant science *5*, 83.

Fierz, B., Chatterjee, C., McGinty, R.K., Bar-Dagan, M., Raleigh, D.P., and Muir, T.W. (2011). Histone H2B ubiquitylation disrupts local and higher-order chromatin compaction. Nat Chem Biol *7*, 113-119.

Fleming, A.B., Kao, C.F., Hillyer, C., Pikaart, M., and Osley, M.A. (2008). H2B ubiquitylation plays a role in nucleosome dynamics during transcription elongation. Mol Cell *31*, 57-66.

Fleury, D., Himanen, K., Cnops, G., Nelissen, H., Boccardi, T.M., Maere, S., Beemster, G.T., Neyt, P., Anami, S., Robles, P.*, et al.* (2007). The Arabidopsis thaliana homolog of yeast BRE1 has a function in cell cycle regulation during early leaf and root growth. Plant Cell *19*, 417-432.

Gardner, R.G., Nelson, Z.W., and Gottschling, D.E. (2005). Ubp10/Dot4p regulates the persistence of ubiquitinated histone H2B: distinct roles in telomeric silencing and general chromatin. Molecular and cellular biology *25*, 6123-6139.

Grant, P.A., Duggan, L., Cote, J., Roberts, S.M., Brownell, J.E., Candau, R., Ohba, R., Owen-Hughes, T., Allis, C.D., Winston, F.*, et al.* (1997). Yeast Gcn5 functions in two multisubunit complexes to acetylate nucleosomal histones: characterization of an Ada complex and the SAGA (Spt/Ada) complex. Genes & development *11*, 1640-1650.

Grasser, M., and Grasser, K.D. (2017). The plant RNA polymerase II elongation complex: A hub coordinating transcript elongation and mRNA processing. Transcription, 1-6.

Henry, K.W., Wyce, A., Lo, W.S., Duggan, L.J., Emre, N.C., Kao, C.F., Pillus, L., Shilatifard, A., Osley, M.A., and Berger, S.L. (2003). Transcriptional activation via sequential histone H2B ubiquitylation and deubiquitylation, mediated by SAGA-associated Ubp8. Genes Dev *17*, 2648-2663.

Holm, L., and Laakso, L.M. (2016). Dali server update. Nucleic acids research *44*, W351-355.

Irigoyen, M.L., Iniesto, E., Rodriguez, L., Puga, M.I., Yanagawa, Y., Pick, E., Strickland, E., Paz-Ares, J., Wei, N., De Jaeger, G.*, et al.* (2014). Targeted degradation of abscisic acid receptors is mediated by the ubiquitin ligase substrate adaptor DDA1 in Arabidopsis. The Plant cell *26*, 712-728.

Jeusset, L.M., and McManus, K.J. (2017). Ubiquitin Specific Peptidase 22 Regulates Histone H2B Mono-Ubiquitination and Exhibits Both Oncogenic and Tumor Suppressor Roles in Cancer. Cancers *9*.

Kelley, L.A., Mezulis, S., Yates, C.M., Wass, M.N., and Sternberg, M.J. (2015). The Phyre2 web portal for protein modeling, prediction and analysis. Nature protocols *10*, 845-858.

Kohler, A., Pascual-Garcia, P., Llopis, A., Zapater, M., Posas, F., Hurt, E., and Rodriguez-Navarro, S. (2006). The mRNA export factor Sus1 is involved in Spt/Ada/Gcn5 acetyltransferase-mediated H2B deubiquitinylation through its interaction with Ubp8 and Sgf11. Molecular biology of the cell *17*, 4228-4236.

Kohler, A., Schneider, M., Cabal, G.G., Nehrbass, U., and Hurt, E. (2008). Yeast Ataxin-7 links histone deubiquitination with gene gating and mRNA export. Nature cell biology *10*, 707-715.

Kohler, A., Zimmerman, E., Schneider, M., Hurt, E., and Zheng, N. (2010). Structural basis for assembly and activation of the heterotetrameric SAGA histone H2B deubiquitinase module. Cell *141*, 606-617.

Lau, O.S., and Deng, X.W. (2012). The photomorphogenic repressors COP1 and DET1: 20 years later. Trends Plant Sci *17*, 584-593.

Lau, O.S., Huang, X., Charron, J.B., Lee, J.H., Li, G., and Deng, X.W. (2011). Interaction of Arabidopsis DET1 with CCA1 and LHY in mediating transcriptional repression in the plant circadian clock. Mol Cell *43*, 703-712.

Lee, K.K., Florens, L., Swanson, S.K., Washburn, M.P., and Workman, J.L. (2005). The deubiquitylation activity of Ubp8 is dependent upon Sgf11 and its association with the SAGA complex. Mol Cell Biol *25*, 1173-1182.

Lee, K.K., Swanson, S.K., Florens, L., Washburn, M.P., and Workman, J.L. (2009). Yeast Sgf73/Ataxin-7 serves to anchor the deubiquitination module into both SAGA and Slik(SALSA) HAT complexes. Epigenetics & chromatin *2*, 2.

Lenstra, T.L., Benschop, J.J., Kim, T., Schulze, J.M., Brabers, N.A., Margaritis, T., van de Pasch, L.A., van Heesch, S.A., Brok, M.O., Groot Koerkamp, M.J.*, et al.* (2011). The specificity and topology of chromatin interaction pathways in yeast. Molecular cell *42*, 536-549.

Li, B., Carey, M., and Workman, J.L. (2007). The role of chromatin during transcription. Cell *128*, 707-719.

Lim, S., Kwak, J., Kim, M., and Lee, D. (2013). Separation of a functional deubiquitylating module from the SAGA complex by the proteasome regulatory particle. Nature communications *4*, 2641.

Liu, Y., Koornneef, M., and Soppe, W.J. (2007). The absence of histone H2B monoubiquitination in the Arabidopsis hub1 (rdo4) mutant reveals a role for chromatin remodeling in seed dormancy. Plant Cell *19*, 433-444.

Love, M.I., Huber, W., and Anders, S. (2014). Moderated estimation of fold change and dispersion for RNA-seq data with DESeq2. Genome biology *15*, 550.

Luo, M., Luo, M.Z., Buzas, D., Finnegan, J., Helliwell, C., Dennis, E.S., Peacock, W.J., and Chaudhury, A. (2008). UBIQUITIN-SPECIFIC PROTEASE 26 is required for seed development and the repression of PHERES1 in Arabidopsis. Genetics *180*, 229-236.

Ma, L., Zhao, H., and Deng, X.W. (2003). Analysis of the mutational effects of the COP/DET/FUS loci on genome expression profiles reveals their overlapping yet not identical roles in regulating Arabidopsis seedling development. Development *130*, 969-981.

Manzano, C., Abraham, Z., Lopez-Torrejon, G., and Del Pozo, J.C. (2008). Identification of ubiquitinated proteins in Arabidopsis. Plant molecular biology *68*, 145-158.

March, E., and Farrona, S. (2017). Plant Deubiquitinases and Their Role in the Control of Gene Expression Through Modification of Histones. Frontiers in plant science *8*, 2274.

Martinez, E., Palhan, V.B., Tjernberg, A., Lymar, E.S., Gamper, A.M., Kundu, T.K., Chait, B.T., and Roeder, R.G. (2001). Human STAGA complex is a chromatin-acetylating transcription coactivator that interacts with pre-mRNA splicing and DNA damage-binding factors in vivo. Molecular and cellular biology *21*, 6782-6795.

Maxwell, B.B., Andersson, C.R., Poole, D.S., Kay, S.A., and Chory, J. (2003). HY5, Circadian Clock-Associated 1, and a cis-element, DET1 dark response element, mediate DET1 regulation of chlorophyll a/b-binding protein 2 expression. Plant Physiol *133*, 1565-1577.

Minsky, N., Shema, E., Field, Y., Schuster, M., Segal, E., and Oren, M. (2008). Monoubiquitinated H2B is associated with the transcribed region of highly expressed genes in human cells. Nat Cell Biol *10*, 483-488.

Misera, S., Muller, A.J., Weiland-Heidecker, U., and Jurgens, G. (1994). The FUSCA genes of Arabidopsis: negative regulators of light responses. Mol Gen Genet *244*, 242-252.

Moraga, F., and Aquea, F. (2015). Composition of the SAGA complex in plants and its role in controlling gene expression in response to abiotic stresses. Frontiers in plant science *6*, 865.

Orlando, D.A., Chen, M.W., Brown, V.E., Solanki, S., Choi, Y.J., Olson, E.R., Fritz, C.C., Bradner, J.E., and Guenther, M.G. (2014). Quantitative ChIP-Seq normalization reveals global modulation of the epigenome. Cell reports *9*, 1163-1170.

Osterlund, M.T., Hardtke, C.S., Wei, N., and Deng, X.W. (2000). Targeted destabilization of HY5 during light-regulated development of Arabidopsis. Nature *405*, 462-466.

Pavri, R., Zhu, B., Li, G., Trojer, P., Mandal, S., Shilatifard, A., and Reinberg, D. (2006). Histone H2B monoubiquitination functions cooperatively with FACT to regulate elongation by RNA polymerase II. Cell *125*, 703-717.

Pepper, A., Delaney, T., Washburn, T., Poole, D., and Chory, J. (1994). DET1, a negative regulator of light-mediated development and gene expression in arabidopsis, encodes a novel nuclear-localized protein. Cell *78*, 109-116.

Perrella, G., and Kaiserli, E. (2016). Light behind the curtain: photoregulation of nuclear architecture and chromatin dynamics in plants. The New phytologist *212*, 908-919.

Peschke, F., and Kretsch, T. (2011). Genome-wide analysis of light-dependent transcript accumulation patterns during early stages of Arabidopsis seedling deetiolation. Plant Physiol *155*, 1353-1366.

Pick, E., Lau, O.S., Tsuge, T., Menon, S., Tong, Y., Dohmae, N., Plafker, S.M., Deng, X.W., and Wei, N. (2007). Mammalian DET1 regulates Cul4A activity and forms stable complexes with E2 ubiquitin-conjugating enzymes. Mol Cell Biol *27*, 4708-4719.

Poullet, P., Carpentier, S., and Barillot, E. (2007). myProMS, a web server for management and validation of mass spectrometry-based proteomic data. Proteomics *7*, 2553-2556.

Rodriguez-Navarro, S. (2009). Insights into SAGA function during gene expression. EMBO Rep *10*, 843-850.

Rodriguez-Navarro, S., Fischer, T., Luo, M.J., Antunez, O., Brettschneider, S., Lechner, J., Perez-Ortin, J.E., Reed, R., and Hurt, E. (2004). Sus1, a functional component of the SAGA histone acetylase complex and the nuclear pore-associated mRNA export machinery. Cell *116*, 75-86.

Roudier, F., Ahmed, I., Berard, C., Sarazin, A., Mary-Huard, T., Cortijo, S., Bouyer, D., Caillieux, E., Duvernois-Berthet, E., Al-Shikhley, L*., et al.* (2011). Integrative epigenomic mapping defines four main chromatin states in Arabidopsis. Embo J *30*, 1928-1938.

Samara, N.L., Datta, A.B., Berndsen, C.E., Zhang, X., Yao, T., Cohen, R.E., and Wolberger, C. (2010). Structural insights into the assembly and function of the SAGA deubiquitinating module. Science *328*, 1025-1029.

Samara, N.L., Ringel, A.E., and Wolberger, C. (2012). A role for intersubunit interactions in maintaining SAGA deubiquitinating module structure and activity. Structure *20*, 1414-1424.

Schmitz, R.J., Tamada, Y., Doyle, M.R., Zhang, X., and Amasino, R.M. (2009). Histone H2B deubiquitination is required for transcriptional activation of FLOWERING LOCUS C and for proper control of flowering in Arabidopsis. Plant Physiol *149*, 1196-1204.

Scholl, R.L., May, S.T., and Ware, D.H. (2000). Seed and molecular resources for Arabidopsis. Plant physiology *124*, 1477-1480.

Schroeder, D.F., Gahrtz, M., Maxwell, B.B., Cook, R.K., Kan, J.M., Alonso, J.M., Ecker, J.R., and Chory, J. (2002). De-etiolated 1 and damaged DNA binding protein 1 interact to regulate Arabidopsis photomorphogenesis. Curr Biol *12*, 1462-1472.

Selth, L.A., Sigurdsson, S., and Svejstrup, J.Q. (2010). Transcript Elongation by RNA Polymerase II. Annual review of biochemistry *79*, 271-293.

Seluzicki, A., Burko, Y., and Chory, J. (2017). Dancing in the dark: darkness as a signal in plants. Plant, cell & environment *40*, 2487-2501.

Shema, E., Tirosh, I., Aylon, Y., Huang, J., Ye, C., Moskovits, N., Raver-Shapira, N., Minsky, N., Pirngruber, J., Tarcic, G*., et al.* (2008). The histone H2B-specific ubiquitin ligase RNF20/hBRE1 acts as a putative tumor suppressor through selective regulation of gene expression. Genes Dev *22*, 2664-2676.

Smith, E., and Shilatifard, A. (2013). Transcriptional elongation checkpoint control in development and disease. Genes & development *27*, 1079-1088.

Sridhar, V.V., Kapoor, A., Zhang, K., Zhu, J., Zhou, T., Hasegawa, P.M., Bressan, R.A., and Zhu, J.K. (2007). Control of DNA methylation and heterochromatic silencing by histone H2B deubiquitination. Nature *447*, 735-738.

Srivastava, R., Rai, K.M., Pandey, B., Singh, S.P., and Sawant, S.V. (2015). Spt-Ada-Gcn5-Acetyltransferase (SAGA) Complex in Plants: Genome Wide Identification, Evolutionary Conservation and Functional Determination. PloS one *10*, e0134709.

Sullivan, A.M., Arsovski, A.A., Lempe, J., Bubb, K.L., Weirauch, M.T., Sabo, P.J., Sandstrom, R., Thurman, R.E., Neph, S., Reynolds, A.P*., et al.* (2014). Mapping and dynamics of regulatory DNA and transcription factor networks in A. thaliana. Cell reports *8*, 2015-2030.

Tamayo, A.G., Duong, H.A., Robles, M.S., Mann, M., and Weitz, C.J. (2015). Histone monoubiquitination by Clock-Bmal1 complex marks Per1 and Per2 genes for circadian feedback. Nature structural & molecular biology *22*, 759-766.

Thorvaldsdottir, H., Robinson, J.T., and Mesirov, J.P. (2013). Integrative Genomics Viewer (IGV): high-performance genomics

data visualization and exploration. Briefings in bioinformatics *14*, 178-192.

Traas, J.A., Doonan, J.H., Rawlins, D.J., Shaw, P.J., Watts, J., and Lloyd, C.W. (1987). An actin network is present in the cytoplasm throughout the cell cycle of carrot cells and associates with the dividing nucleus. The Journal of cell biology *105*, 387-395.

Van Leene, J., Eeckhout, D., Cannoot, B., De Winne, N., Persiau, G., Van De Slijke, E., Vercruysse, L., Dedecker, M., Verkest, A., Vandepoele, K.*, et al.* (2015). An improved toolbox to unravel the plant cellular machinery by tandem affinity purification of Arabidopsis protein complexes. Nature protocols *10*, 169-187.

Van Lijsebettens, M., and Grasser, K.D. (2014). Transcript elongation factors: shaping transcriptomes after transcript initiation. Trends in plant science *19*, 717-726.

Vlachonasios, K.E., Thomashow, M.F., and Triezenberg, S.J. (2003). Disruption mutations of ADA2b and GCN5 transcriptional adaptor genes dramatically affect Arabidopsis growth, development, and gene expression. Plant Cell *15*, 626-638.

Weake, V.M., Lee, K.K., Guelman, S., Lin, C.H., Seidel, C., Abmayr, S.M., and Workman, J.L. (2008). SAGA-mediated H2B deubiquitination controls the development of neuronal connectivity in the Drosophila visual system. Embo J *27*, 394-405.

Weake, V.M., and Workman, J.L. (2008). Histone ubiquitination: triggering gene activity. Mol Cell *29*, 653-663.

Weake, V.M., and Workman, J.L. (2011). SAGA function in tissue-specific gene expression. Trends Cell Biol.

Wertz, I.E., O'Rourke, K.M., Zhang, Z., Dornan, D., Arnott, D., Deshaies, R.J., and Dixit, V.M. (2004). Human De-etiolated-1 regulates c-Jun by assembling a CUL4A ubiquitin ligase. Science *303*, 1371-1374.

Wu, S.H. (2014). Gene expression regulation in photomorphogenesis from the perspective of the central dogma. Annual review of plant biology *65*, 311-333.

Wyce, A., Xiao, T., Whelan, K.A., Kosman, C., Walter, W., Eick, D., Hughes, T.R., Krogan, N.J., Strahl, B.D., and Berger, S.L. (2007). H2B ubiquitylation acts as a barrier to Ctk1 nucleosomal recruitment prior to removal by Ubp8 within a SAGA-related complex. Mol Cell *27*, 275-288.

Xin, H., Takahata, S., Blanksma, M., McCullough, L., Stillman, D.J., and Formosa, T. (2009). yFACT induces global accessibility of nucleosomal DNA without H2A-H2B displacement. Mol Cell *35*, 365-376.

Yanagawa, Y., Sullivan, J.A., Komatsu, S., Gusmaroli, G., Suzuki, G., Yin, J., Ishibashi, T., Saijo, Y., Rubio, V., Kimura, S.*, et al.* (2004). Arabidopsis COP10 forms a complex with DDB1 and DET1 in vivo and enhances the activity of ubiquitin conjugating enzymes. Genes Dev *18*, 2172-2181.

Zeng, M., Ren, L., Mizuno, K., Nestoras, K., Wang, H., Tang, Z., Guo, L., Kong, D., Hu, Q., He, Q.*, et al.* (2016). CRL4(Wdr70) regulates H2B monoubiquitination and facilitates Exo1-dependent resection. Nature communications *7*, 11364.

Zimmermann, L., Stephens, A., Nam, S.Z., Rau, D., Kubler, J., Lozajic, M., Gabler, F., Soding, J., Lupas, A.N., and Alva, V. (2017). A Completely Reimplemented MPI Bioinformatics Toolkit with a New HHpred Server at its Core. Journal of molecular biology.